JOURNAL OF MATERIALS SCIENCE 21 (1986) 2908–2914

A porous material prepared from the layer-type complex consisting of montmorillonite and α-naphthylamine

A. ŌYA, H. YASUDA, A. IMURA, S. ŌTANI
Faculty of Engineering, Gunma University, Kiryu, Gunma 376, Japan

Aqueous mixtures of montmorillonite and α-naphthylamine with various mixing ratios were kept at 353 K for 3 days with stirring to convert them into the layer-type complex (MNC) consisting of both components, and then dried at 403 K. The resulting blocks, several centimetres in size, were heated below 1473 K under nitrogen. The addition of α-naphthylamine (NA) in the equivalent amount to the cation exchange capacity of montmorillonite resulted in the most attractive porous material which includes homogeneous pores of ~35 nm radius and exhibits a maximum pore volume of 0.8 ml g^{-1} at 873 K. The samples containing greater and lesser amounts of NA gave a very brittle block and a less porous block after heating to high temperature, respectively. The materials obtained were also characterized by the waved card-house structure. The amount of NA added and the heat-treatment temperature did not vary the pore size so widely.

1. Introduction

The present authors have previously reported the thermal degradation behaviour of a layer-type complex (MNC) consisting of montmorillonite (Mont) and α-naphthylamine (NA), in which the following points were noted, (i) thermal stability of the layered structure of MNC was superior than that of raw Mont by about 200 K, and (ii) a porous material with the waved card-house structure may be prepared easily using MNC [1, 2].

The present work was carried out to characterize the porous material from MNC in further detail. The effects of the amount of NA added at the MNC formation process and of the heat-treatment temperature (HTT) on the resulting porous material were examined in detail.

2. Experimental details

2.1. Preparation and heat-treatment procedures of MNC

Raw Mont from Aterasawa, Yamagata, Japan was kindly supplied by Kunimine Ind. Co Ltd. Mont particles of smaller than 2 to 3 μm in size, were collected by the usual sedimentation technique and served for the present work without homoionization. This Mont has a cation exchange capacity (CEC) of 108.3 meq/100 g and the chemical formula is

$$M(Al_{3.40}Fe^{3+}_{0.09}Fe^{2+}_{0.06}Mg_{0.47})$$
$$(Si_{7.65}Al_{0.35})O_{20}(OH)_4 \cdot nH_2O$$

where M is alkali metal.

α-naphthylamine hydrochloride($C_{10}H_7NH_2 \cdot HCl$) was added to several per cent Mont aqueous sol to give solutions with 0.50, 0.75, 1.00, 1.25 and 1.50 times the CEC of Mont, followed by keeping at 353 K for 3 days to convert it into MNCs intercalated with various amounts of NA. The resultant MNCs are shown by fixing the amount of NA added, e.g. 0.50 MNC and 1.25 MNC. The MNC sol was concentrated by centrifuging, followed by preparation into a film of several 10 μm thick and a block several centimetres in size, through drying at 403 K. Finally, both samples were heated to fixed temperatures below 1473 K at 5 K min^{-1} and kept for 1 h under nitrogen.

2.2. Measurements

The film sample was used for X-ray diffraction analysis to calculate the basal spacing (d_{001}) of the layered structure and to identify the compounds deposited in MNC at high HTT. Thermogravimetric analysis (TG–DTA) was also carried out using the film sample in a flow of nitrogen or air at a heating rate of 10 K min^{-1}. The fracture surface of the block sample was observed by scanning electron microscopy (SEM). The carbon content in the sample was measured by the combustion method. Here, tin metal particles were added to ensure complete combustion of sample. Pore size distribution was determined using a mercury porosimeter. The gases evolved from the MNC block during the heating process were analysed quantitatively at intervals of 50 K; further details are reported elsewhere [3].

3. Results

3.1. X-ray diffraction analysis

X-ray diffraction profiles of some MNC samples and basal spacings are shown in Figs 1 to 3 and Table I. As can be seen from Fig. 1, 0.50 MNC gave the composite (0 0 1) diffraction profile around 6° (2θ, Cu$K\alpha$), which indicates the co-existence of both Mont and MNC,

0022–2461/86 $03.00 + .12

TABLE I Changes of basal spacings (nm) with HTT

HTT (K)	Li-Mont	0.50MNC	0.75MNC	1.00MNC	1.25MNC	1.50MNC
Orig.	1.23	1.52	1.55	1.61	1.61	1.61
673	0.96	1.42	1.28	1.45	1.52	1.55
873	0.95	0.96	1.00	1.30	1.45	1.12
1073	0.95	0.98	0.98	1.23	1.03	1.03
1273	*	*	*	1.38	*	*
1473	*	*	*	*	*	*

*The layered structure was destroyed completely.

because of insufficient addition of NA. Table I shows the average basal spacing. Based on these X-ray diffraction data, the intercalated NA in 0.50MNC is removed around 873 K, followed by similar thermal degradation behaviour to that of Li-Mont at higher HTT [1]. After destruction of the MNC structure, the deposited compounds were found to be magnesium aluminium silicate ($MgO \cdot Al_2O_3 \cdot xSiO_2$, $x = 3$ or 4, abbreviation: MAS) at 1273 K, and mullite ($3Al_2O_3 \cdot 2SiO_2$) and cordierite ($2MgO \cdot 2Al_2O_3 \cdot 5SiO_2$) at 1473 K, respectively. As can be suggested from the complex chemical formula of raw Mont, these compounds may or may not have such stoichiometric formulae. 0.75MNC exhibited very similar behaviour to this although not presented here. 1.00MNC alone shows diffraction peaks resulting from the layered structure even after heating to 1273 K, but the compounds deposited at 1473 K were mullite and cordierite, as well as 0.50MNC. 1.25MNC exhibited a similar behaviour to that shown in Fig. 3 for 1.50MNC, namely, both samples decreased their basal spacings gradually up to 1073 K and were destroyed completely at 1273 K to yield mullite and quartz (SiO_2) which further changed into cristobalite (SiO_2) at 1473 K.

3.2. Carbon content

The carbon contents for some samples are shown in Table II. The contents in the original samples increased with increasing addition of NA. This trend was also retained after heating to a higher HTT, except for 1.50MNC.

3.3. TG-DTA

Fig. 4 shows TG-DTA curves in the flow of nitrogen. The weight decreases just below 400 K and about 1000 K are due to the dehydration of the interlayer water and hydroxyl groups. The difference between the three MNC samples became clearer, especially around 700 to 1100 K, in the flow of air as shown in Fig. 5. 0.50MNC, 1.00MNC and 1.50MNC exhibited no, one and two exothermic peaks accompanied by a weight decrease in this temperautre range, respectively.

3.4. Analysis of the evolved gases

The quantitative analysis of the gases evolved from 1.00MNC and 1.50MNC are shown in Figs 6 and 7. Remarkably, H_2O evolved from 1.00MNC around 350 and 850 K, which is attributable to dehydration of the interlayer water and hydroxyl groups observed in the thermogravimetric analysis. Hydrogen began to evolve around 850 K and reached a maximum at 1000 K. Compared with these gases, CO and CH_4 evolved much less. 1.50MNC exhibited some small differences from 1.00MNC, namely, hydrogen evolved at a slightly lower temperature and the amount of hydrogen evolved was relatively little, although hydrogen may evolve at a higher temperature than 1273 K.

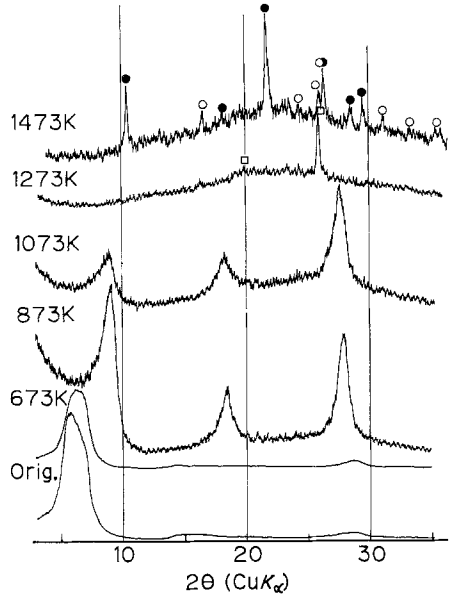

Figure 1 Change of X-ray diffraction profiles of 0.50MNC with HTT. ○ Mullite, ● cordierite, □ MAS.

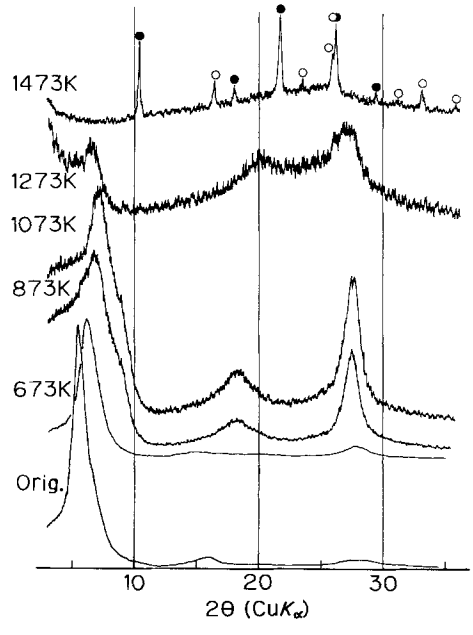

Figure 2 Change of X-ray diffraction profiles of 1.00MNC with HTT. ○ Mullite, ● cordierite.

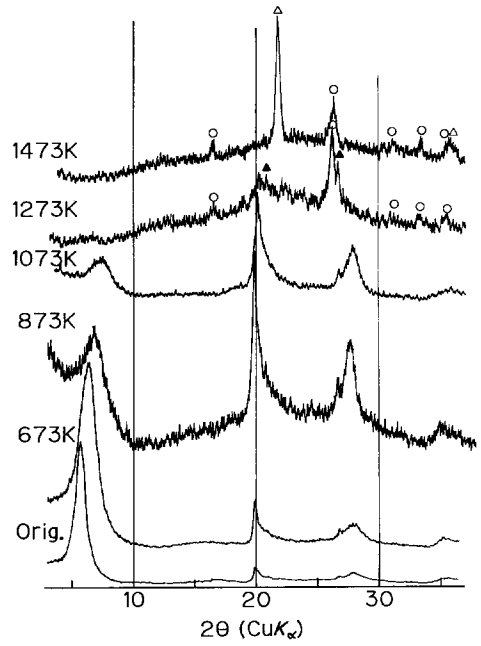

Figure 3 Change of X-ray diffraction profiles of 1.50MNC with HTT. ○ Mullite, △ cristobalite, ▲ quartz.

3.5. SEM observations

The fracture surfaces of 0.50MNC, 1.00MNC and 1.50MNC are shown in Figs 8, 9 and 10. 0.75MNC and 1.25MNC, which are not shown, exhibited intermediate appearances between the former two and the latter two MNCs, respectively. 0.50MNC after heating to 673 K exhibited a clear wave card-house structure but became more dense on sintering at higher HTT. As shown in Fig. 9, sintering was also observed in 1.00MNC but the porous structure was maintained up to higher HTT. 1.50MNC resulted in a porous block which was too brittle to retain its entity. This MNC maintained a porous structure up to the highest HTT from comparison of scanning electron micrographs.

3.6. Pore size distribution

Taking into account SEM observations stated above, 1.00MNC and 1.25MNC were used for pore size distribution measurements which are shown in Figs 11 and 12. Table III shows the pore value, average pore radius and pore radii at 20% and 80% of the pore volume, for evaluation of the homogeneity of the pores. Both MNCs exhibited maximum pore volumes at 873 K and smaller volumes at higher HTT. A

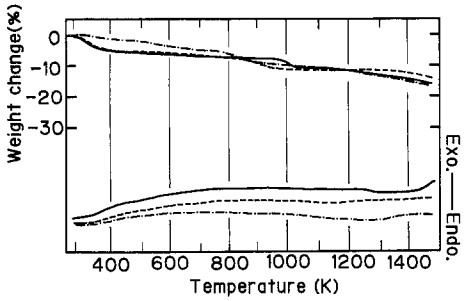

Figure 4 TG–DTA curves of some MNCs in the flow of nitrogen (heting rate: 10 K min^{-1}). ——— 0.50MNG, ---- 1.00MNG, -·-·- 1.50MNG.

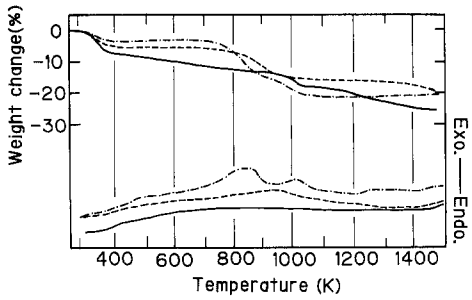

Figure 5 TG–DTA curves of some MNCs in the flow of air (heating rate: 10 K min^{-1}). ——— 0.50MNG, ---- 1.00MNG, -·-·- 1.50MNG.

remarkable decrease in the pore volume was observed between 1073 and 1273 K. The average pore radii of 1.00MNC and 1.25MNC were 34 and 27 nm, respectively. These pore radii changed little with HTT. Here it should be emphasized that these pore size distributions are quite narrow.

4. Discussion

4.1. Characteristics of the present preparation method and of the porous material obtained

There are some methods of microporous material (ceramics) preparation, including a similar size of pores to those of the present material, e.g. (i) to mould the fibre or the particle with or without the binder – the ceramic filter [4], (ii) to remove some component preferentially from the heterogeneous components material – porous glass [5], silica gel [6], of which details can be found elsewhere. Compared with these methods, the present preparation procedure is quite simple as stated above, which is the most important feature of this method.

It is thought that MNC leads to such a simple preparation method because when raw Mont was subjected to the same processes, it resulted in no block, but the film or the thin plate oriented along the glass container wall. The size of the pores developed after heating was also very heterogeneous, details of which have been reported previously [2]. Mont particle,

TABLE II Changes of carbon content (wt %) with HTT

HTT (K)	0.50MNC	0.75MNC	1.00MNC	1.25MNC	1.50MNC
Orig.	6.0	7.2	11.1	12.6	13.8
1073	5.5	7.6	11.2	15.2	13.1
1273	4.6	7.4	10.0	14.3	12.0

TABLE III Pore volumes and average pore radii

HTT (K)	1.00MNC		1.25MNC	
	Pore volume (ml g^{-1})	Pore radius (nm)	Pore volume (ml g^{-1})	Pore radius (nm)
Orig.	0.643	34(24–44)	0.514	26(15–42)
673	0.679	34(23–43)	0.533	27(15–40)
873	0.777	34(24–44)	0.613	28(16–42)
1073	0.764	33(22–43)	0.534	28(15–43)
1273	0.403	35(22–46)	0.478	26(16–42)

( ): pore radii at pore volume × 0.8 and × 0.2.

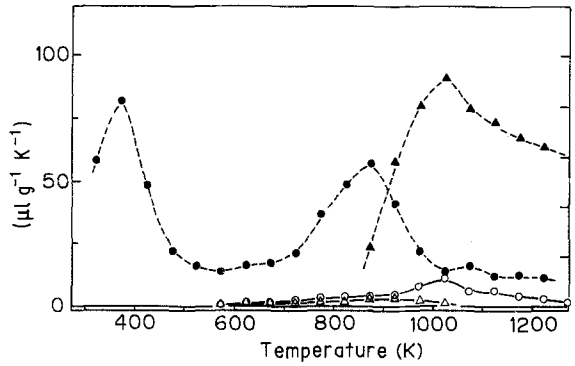

Figure 6 Analysis of the gases evolved from 1.00 MNC. ○ CO, ● H_2O, △ CH_4, ▲ H_2.

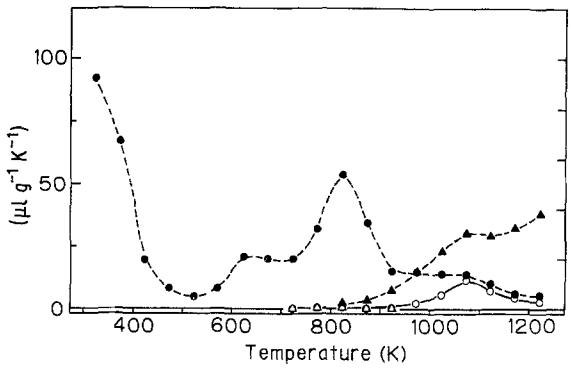

Figure 7 Analysis of the gases evolved from 1.25 MNC. ○ CO, ● H_2O, △ CH_4, ▲ H_2.

possible, has too large an anisotropy in shape to maintain the card-house structure after drying, but the anisotropy is lowered adequately by intercalating with NA, leading to the stable card-house structure retained even after heating to high HTT.

The structure of this porous material is characterized macroscopically by the waved card-house structure and microscopically by the layer-type complex of Mont/NA (the carbon reside after heating to high HTT). Such characteristic structures govern the properties of the resulting material; for example, the porous structure consisting of the thin cards leads to a large pore volume. The narrow pore size distribution stated above may also result from the homogeneity in size of the Mont cards. In addition, this porous material is expected to have a high mechanical strength because of its honeycomb-like structure, which will be reported later. The microscopic structural feature of the layer-type complex may affect such properties as chemical resistivity. Here one problem is the low oxidation resistivity of the layer-type complex because of the lack of rigid bonding between the carbon and Mont layer, except for the 1273 K MNC [7]. Therefore, some limitations must be put on the use of this porous material under oxidative atmospheres at high temperature.

4.2. Thermal degradation behaviour of NA

Between 0.50 MNC and 1.00 MNC, the amount of intercalated NA increased with increasing of addition of NA (Figs 1 to 3 and Table I). However, combustion of 1.50 MNC consists of two steps, as shown in Fig. 5. Thus, additional NA to the equivalent amount of CEC of raw Mont cannot intercalate, but just attaches to the Mont particle surface. At the heat-treatment process, as stated previously [1], the intercalated NA

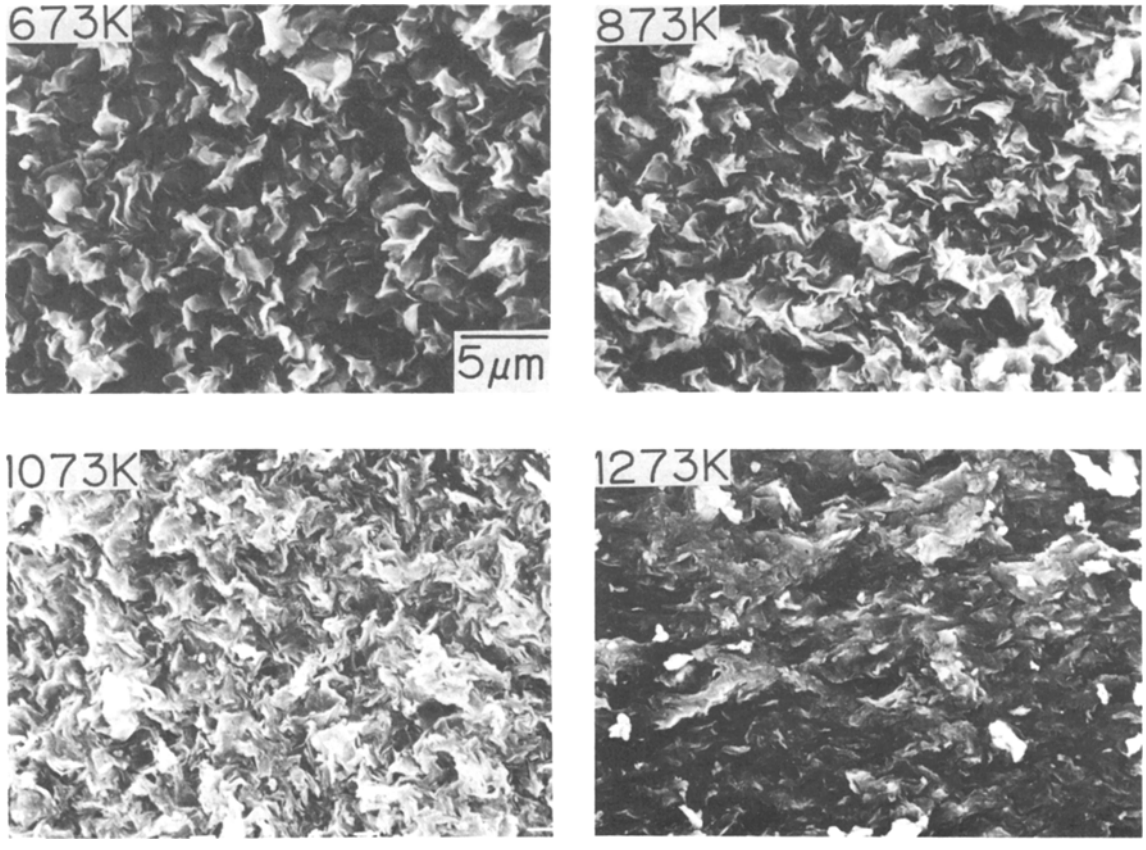

Figure 8 Scanning electron micrographs of 0.50 MNC.

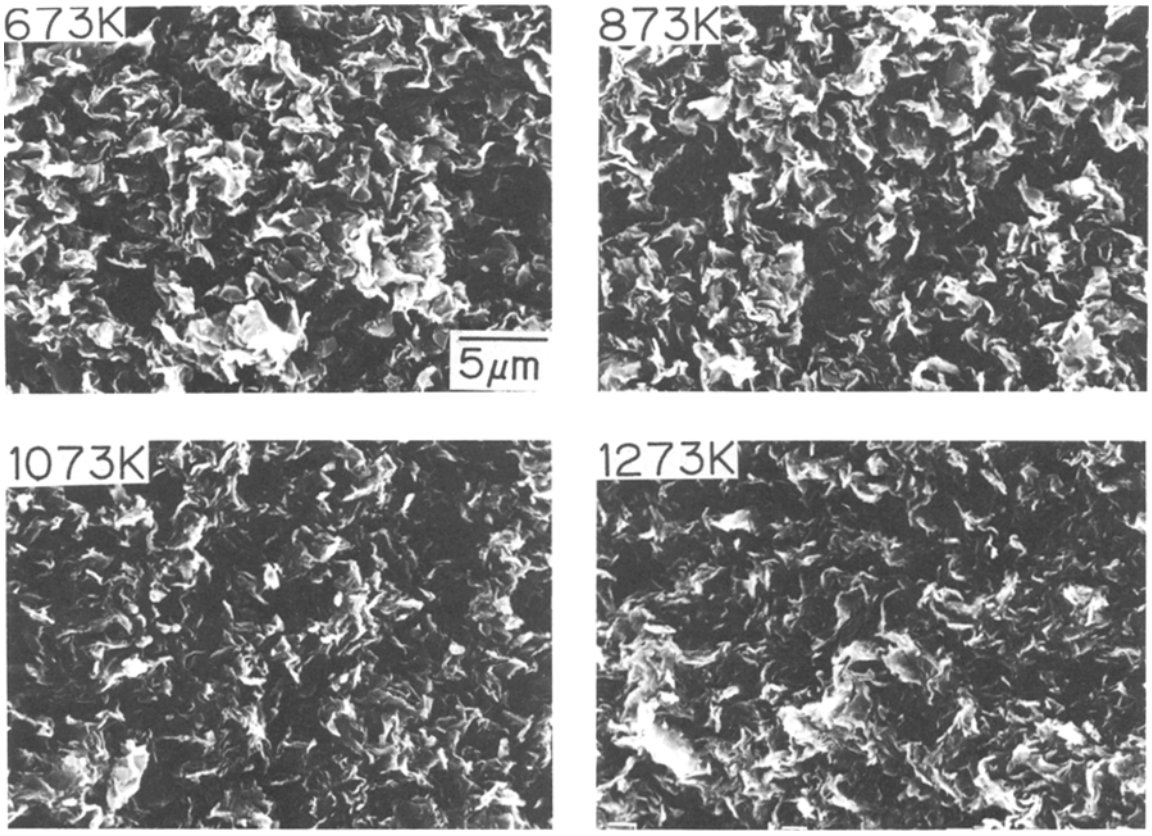

Figure 9 Scanning electron micrographs of 1.00 MNC.

is partially removed as NA itself, but mostly carbonizes to result in an imperfect carbon layer, leading to an improvement of the thermal stability of the layered structure of MNC through disturbing the sintering. Since carbonization of NA must evolve hydrogen, such a process proceeds abruptly above 800 K (Figs 6 and 7). The improvement of the thermal stability of the organic compound by intercalating has also been reported elsewhere [8].

Another point to be noted here is that the layered structures of 1.25 MNC and 1.50 MNC are less stable than that of 1.00 NMC. The reason is not clear at

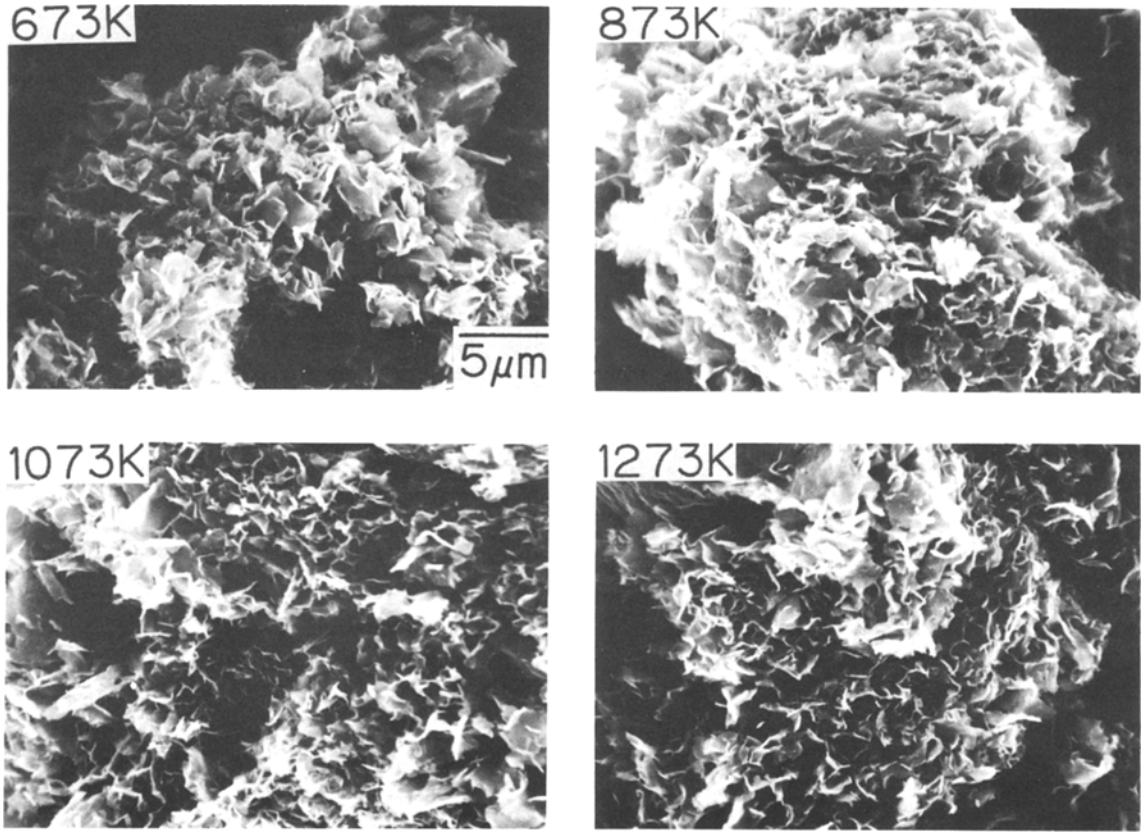

Figure 10 Scanning electron micrographs of 1.50 MNC.

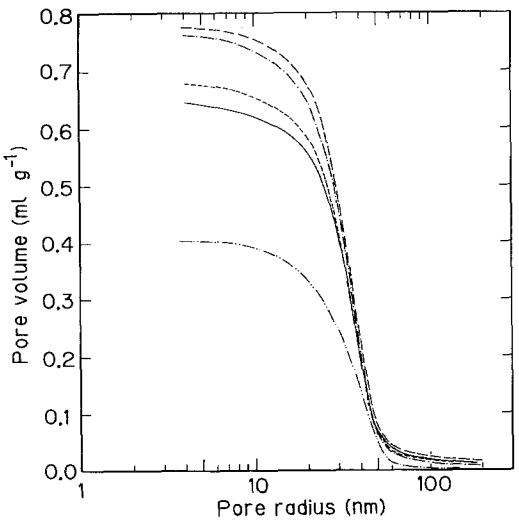

Figure 11 Pore size distribution diagrams of 1.00MNC heated to various HTTs. —— Original, ---- 673 K, --- 873 K, -·-·- 1073 K, -··-··- 1273 K.

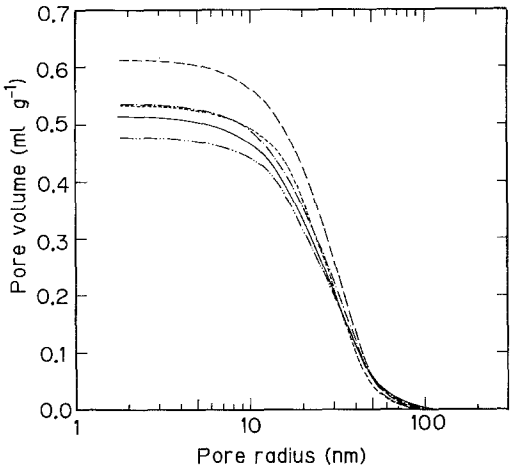

Figure 12 Pore size distribution diagrams of 1.25MNC heated to various HTTs. —— Original, ---- 673 K, --- 873 K, -·-·- 1073 K, -··-··- 1273 K.

present, but one possibility is the reduction of Mont by additional carbon.

4.3. Effect of amount of Na added and HTT on the porous structure

The structure of the present porous material will be controlled by (i) the particle size of raw Mont, (ii) the amount of intercalated NA in Mont, (ii) drying conditions of MNC sol and heat-treatment conditions of MNC block. The effects of addition of NA and HTT are examined here.

4.3.1. Effects of addition amount of NA

As can be seen from the scanning electron micrographs a large amount of NA added lowered the sinterability of the resulting MNC block. The lowering observed between 0.50MNC and 1.00MNC is attributable to the formation of a more extensive carbon layer between the Mont layers, leading to more serious interference to sintering. This idea will be supported by the carbon contents shown in Table II. The lowering of sintering between 1.00MNC and 1.50MNC seems to result from other causes. One possible cause is that a more extensive carbon layer was formed in 1.00MNC than in 1.50MNC because of a larger amount of hydrogen evolution in 1.00MNC. However, the layered structure of 1.50MNC is also lowered, that is, the surface carbon should be considered to lower the sinterability through the reaction with MNC, possibly resulting in a low sinterable compound which may be SiO_2 and Al_4C_3 as stated above. We thought initially that the surface carbon may reduce the Mont layer to lower the thermal stability of the layered structure of MNC, but this idea is not reasonable in view of the results shown in Figs 6 and 7. The effects of the amount of NA added on the pore volume and pore size distribution were not so clear, because of the comparison between just two samples. It is reasonable to consider, however, that the pore size is not changed greatly by varying the amount of NA added.

4.3.2. The effects of HTT

The effects of HTT on the porous structure is not necessarily the same for all MNC samples, as can be seen from the scanning electron micrographs. However, a similar tendency was observed in 1.00MNC and 1.25MNC, that is, the pore volume exhibited a maximum at 873 K. Below this HTT, the weight decrease acts mainly to increase the pore volume. As shown in the micrographs, on the contrary, sintering decreases the pore volume at higher HTT. Such a trend seems to occur in the MNC sample with smaller amounts of NA, which was verified between 1.00MNC and 1.50MNC in Figs 11 and 12.

5. Conclusions

1. Just by drying and heating Mont/α-naphthylamine complex (MNC) under nitrogen, a unique porous material was obtained. This material, with a waved card-house structure, consists of homogeneous pores of several 10 nm radius and has a relatively large pore volume.

2. MNC from Mont and an equivalent amount of naphylamine (NA) to the cation exchange capacity of Mont, gave the most attractive porous material. MNC with lesser and greater amounts of NA resulted in a less porous material and a brittle porous material after heating, respectively.

3. The porous material exhibited a maximum pore volume at 873 K but the pore size did not vary so widely with HTT.

Acknowledgements

The authors wish to thank Mr H. Hanaoka of the Gunmaken Industrial Research Laboratory for the carbon content measurement and Dr Y. Yamashita of National Research Insitute for Pollution and Resources for the gas analysis. Thanks are also due to Mr H. Kakegawa of Ibiden Co Ltd and Mr A. Kotato of Hitachi Chemical Ind. Ltd for the pore size distribution measurement. Raw montmorillonite was kindly supplied by Kunimine Ind. Co Ltd.

References

1. A. ŌYA, Y. OMATA and S. ŌTANI, *J. Mater. Sci.* **20** (1985) 255.
2. A. ŌYA, Y. OMATA, K. KIZU and S. ŌTANI, *ibid.* in press.
3. Y. YAMASHITA and K. OUCHI, *Nenryuo Kyoukai-shi* (*J. Fuel Soc. Jpn*) **53** (1974) 1064.
4. N. YAMAMOTO, *Ceramics* **10** (1975) 775.
5. H. P. HOOD and M. E. NORDBERG, US Patents 2215039, 2221709 (1940).
6. R. K. ILER, "The Colloid Chemistry of Silica and Silicates" (Cornell University Press, Ithaca New York, 1955).
7. A. ŌYA, Y. OMATA and S. ŌTANI, *J. Mater. Sci.* **20** (1985) 516.
8. A. BLUMENSTEIN, *J. Polym. Sci. A* **3** (1965) 2665.

Received 23 September
and accepted 12 October 1985